

## Shannon Entropy based Reliability Calculation for Tritium Plasma Retention in Graphene by using Molecular Dynamics

Alper Pahsa, PhD<sup>1</sup>,  
<sup>1</sup>HAVELSAN Inc, Ankara, Turkiye  
Orcid:0000-0002-9576-5297

### Abstract

When choosing reactor components, Tokamak fusion reactor structural reliability must be considered. Fusion reactions, which generate heat and energy, can modify reactor walls. Because of this, reactors generate energy less efficiently. For example, graphene is the principal material used to build fusion reactor walls. Graphene is the latest high-tech substance. The study used molecular dynamics simulations to determine how tritium plasma ions with energy from 5 to 35 keV affected graphene walls. Since molecular dynamics demonstrate a chaotic system surface molecular model, Shannon entropy is employed to determine the surface. This calculation uses Shannon Entropy of the surface and the Weibull distribution to forecast graphene manufacturing reliability.

**Keywords:** PMI Shannon Entropy, material reliability calculation with Shannon Entropy, Weibull Reliability based on Shannon Entropy

---

### 1. INTRODUCTION

Rising population and living standards are boosting energy demand, a major concern this century. Most energy comes from depleting fossils. Sustainability requires nuclear and renewable energy [1-2]. The last stage of exothermic nuclear processes generates energy. Vital nuclear reactions include fission and fusion. An unstable, large nucleus breaking into two or more smaller nuclei releases energy. Most nuclear reactors use fission. Multiple nuclei fuse in nuclear fusion. Nuclear and subatomic particles result. Mass shifts in reactants and products generate energy. Fusing demands 100 million degrees. Nuclear fusion provides nearly infinite fuel worldwide. Fusion reactors create transient radioactive waste with safety measures [3-6]. The most renowned fusion reaction uses

tritium and deuterium. The 14.1 MeV neutron from this event heats water to generate turbine steam. Additionally, this reaction produces 3.5 MeV He [7-10]. Plasma is heated by reactor helium nuclei [11-15]. Traditional thermonuclear fusion reactors densify plasma with magnetic fields. Plasma from the reactor's (Figure 1) first wall is trapped in a magnetic field. Hi-energy plasma affects obstacles. The divertor zone has the highest attrition because magnetic field lines carry lower-energy plasma to the wall. Fusion research examines plasma-first wall materials and interactions.



Figure 1. Internal view of the nuclear fusion reactor (Tokamak)

Fusion helium must be extracted from plasma. Helium interacts with divertor walls during removal [16-18]. Dying divertor and reactor walls release neutrons. Tokamak reactor wall erosion is prevented by tungsten, beryllium, molybdenum, steel, and graphene. High melting point and atomic number make tungsten plasma-resistant [16-19]. Nuclear fission reactor structural reliability analysis is rare in reliability literature. [19] investigates nuclear fission reactor structural system and component lifetime, dependability, and risk assessments. This source uses probability, material science, fluid, fracture, and structural mechanics. Fusion reactions are most nuclear fusion reactors' principal problem. Literature understates structure reliability. In [20], recent structural and thermomechanical studies are presented. Discussing diagnostic, magnet, and reproductive coverage. Safe and reliable systems affect fusion device dependability. Communicating reliability. ITER, DEMO, and Wendelstein 7-X fusion equipment for energy generation or

experiments are tested for availability, maintainability, and inspectability [21]. This study covers only fusion device basics. Commercial plasma applications with surface coating are best for Tokamak fusion reactor structure reliability testing. Space-based plasma-facing structures must resist radiation and particles. Plasma-facing structures must withstand radiation and particles to reduce space impacts [22-24]. Tritium was hard to preserve in Tokamak nuclear fusion reactor walls. Plasma-facing graphene magnetic fusion systems suffer tritium loss. JET and TFTR plasma tritium retention was 40% and 51%. e After experiments, fusion reactor sanitization took 12–16%. Walls of titanium. To According to recent models, the French experimental Tokamak reactor ITER will reach its tritium limit after 100 pulses. Rising tritium levels bend reactor walls, decreasing lifespan. It impacts fusion's thermal-to-electric energy transfer. This study created a graphene wall structure with larger crystal atomic patterns using molecular dynamics simulations. Figure 2 shows the simulation's initial research model.

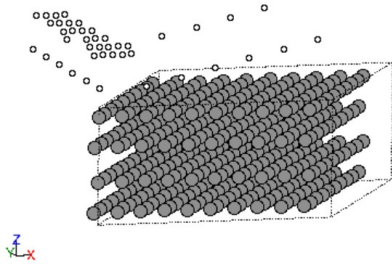


Figure 2. Atomic simulation system startup model configuration for Tritium and Graphene surface crystal

## 2. METHOD

This work modeled the retention mechanism for a sizable amount of graphite, with almost 1,200 carbon atoms. The results implied that the retention efficiency depended on several elements, including the pressure and temperature settings during the simulation. These findings might have important consequences for the next studies on carbon-based materials and their uses in different sectors. We exposed the block to hydrogen at energy levels ranging from 5 to 35 keV (substituting tritium) to enable calculations with 3T electromagnetic force application. These energy levels were sufficient for the simulation, implying that the present simulations cover a reasonable spectrum of collision energy in the literature. The aim of this work was to develop a model using Shannon entropy that would allow tritium production by measuring surface kinetic energy. We would investigate the interaction

between graphite and hydrogen atoms by building this model with molecular dynamics simulations. We execute molecular dynamics simulations using the Python programming language. Spyder (Scientific Python Editor) 6.0.3, which is included in the Anaconda package, is employed for this purpose. The computations are executed on a Dell Precision 7680 with an Intel Core i7 13th Gen processor using the Ubuntu 24.10 Linux operating system. The compiler version of Python was 3.12.7. This study utilizes the molecular dynamics simulation tool, Python-based Atomic Simulation Environment (ASE [25]). This figure 3 explains the molecular dynamic process algorithm of tritium atoms bombarding the graphene crystal structure.

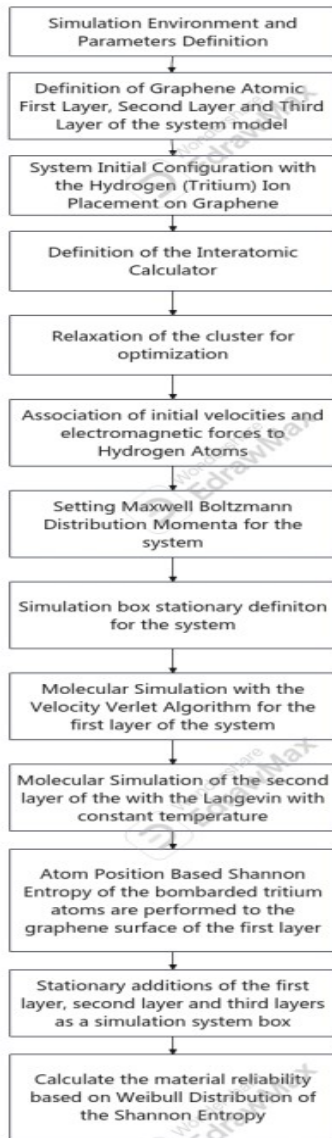


Figure 3. Molecular Dynamics Simulation Process of the Graphene crystal bombarded with the Tritium.

In this simulation based on the atom positions Shannon Entropy is calculated for the system. Shannon explains that the set of probabilities can be found as  $p_1, p_2, p_3, \dots, p_n$ , that produces vagueness via  $(H)$  measurement. When the positions of the atoms given in this system model is carried out the Shannon Entropy is given as [26]:

$$H = K \sum_{i=1}^n p_i \log_2 p_i \quad (1)$$

Equation above (1) gives Shannon Entropy with its probabilities  $p_1, p_2, p_3, \dots, p_n$  that have frequency of the atoms observed inside system configuration atom model in the molecular dynamics. Based on the calculated values of the Shannon Entropy values, reliability distribution of the Weibull is calculated. The three-parameter Weibull distribution equation is given below [27]:

$$R(t) = e^{-\left(\frac{t-\gamma}{a}\right)^\beta} \quad (2)$$

where  $t$  represents the irradiation duration,  $\gamma$  denotes the location parameter,  $\beta$  signifies the shape parameter (slope) with  $\beta > 0$ , and  $\alpha$  indicates the scale parameter (characteristic life) with  $\alpha > 0$ . In calculations, it is widely accepted that  $\gamma = 0$ , as it represents the displacement of the origin of the reliability distribution graph. The failure probability function is defined as:

$$F(t) = 1 - R(t) \quad (3)$$

$$1 - F(t) = e^{-\left(\frac{t}{a}\right)^\beta} \quad (4)$$

In the aforementioned,  $\gamma = 0$ , and according to the specified criteria for  $F(t)$ , it holds that  $0 < F(t) < 1$ . The configuration of the equation follows the specified criteria:

$$\ln\left(\ln\frac{1}{1-F(t)}\right) = \beta \ln t - \beta \ln a \quad (5)$$

To formulate the equation in the configuration of  $y = mx + n$ , the subsequent expression is produced:

$$y(t) = \ln \left( \ln \frac{1}{1 - F(t)} \right), m = \beta \text{ and } n = -\beta \ln \alpha \quad (6)$$

The Bernard Approximation for Median Ranks is employed to compute the unreliability parameters for each failure [31]. Subsequently, we determine the unreliability parameter.

$$F(t) = \text{MedianRank} = \frac{\text{Rank} - 0.3}{N + 0.4} \quad (7)$$

where N is the maximum number of orders in the table set and rank is the order number in the data set table. The values in Tables 2 and 3 are obtained by utilizing the RMS and Sa values from Table 1 in equations (5) and (6). The characteristic equation of the aluminum samples shown in equation (1) is found by using equation (4) to calculate (3) and (2), and by figuring out F(t) and y(t) in Tables 2 and 3.

### 3. RESULTS & DISCUSSION

Running the structure with energies between 5 keV and 35 keV, the simulation subjects the graphene crystal to impacts from H. The method calls for applying molecular dynamics (MD) simulations in the next stage. The graphene construction features several layers for thermostats. This sequence displays the three-dimensional MD simulation outputs, potential, and kinetic energies. Tables 1, 2, 3, and 4 show the times for the simulation process, the calculated Shannon entropy from the molecular simulation model, the rank, the F(t) function, the natural logarithm of Shannon

entropy, the y(t) function related to Shannon entropy, and the reliability based on the y(t) function for tritium hit with kinetic energies between 5 keV and 35 keV.

Table 1. Shannon Entropy F(t) and y(t) values calculated by equations 1, 2, 3, 4, 5, 6 and 7 for Tritium with 5keV bombardment with 3T on Graphene Crystal

Process Time (fs)	Shannon Entropy of the total bulk surface	Rank	F(t)	ln(Shannon)	y(t)_Shannon	Reliability of Shannon Entropy for 5keV Tritium Bombardment
0	5,5	1	0,074 4680 85	1,704748 092	0	1
25	5	2	0,180 8510 64	1,609437 912	0,478642016	0,521357984
50	4,9	3	0,287 2340 43	1,589235 205	0,503018971	0,496981029
75	4,4	4	0,393 6170 21	1,481604 541	0,517039091	0,482960909
100	3,7	5	0,5	1,308332 82	0,526869951	0,473130049
125	3,5	6	0,606 3829 79	1,252762 968	0,5344255	0,4655745
150	3,3	7	0,712 7659 57	1,193922 468	0,540552053	0,459447947
175	3	8	0,819 1489 36	1,098612 289	0,545698368	0,454301632
200	2,3	9	0,925 5319 15	0,832909 123	0,550130946	0,449869054

Table 2. Shannon Entropy F(t) and y(t) values calculated by equations 1, 2, 3, 4, 5, 6 and 7 for Tritium with 15keV bombardment with 3T on Graphene Crystal

Process Time (fs)	Shannon Entropy of the	Rank	F(t)	ln(Shannon)	y(t)_Shannon	Reliability of Shannon Entropy for 15keV Tritium
-------------------	------------------------	------	------	-------------	--------------	--

	total bulk surface					Bombardment
0	5,1	1	0,0744 68085	1,62924054	0	1
25	4,9	2	0,1808 51064	1,589235205	0,3892742 27	0,61072577 3
50	3,5	3	0,2872 34043	1,252762968	0,3939209 23	0,60607907 7
75	2,5	4	0,3936 17021	0,916290732	0,3966372 47	0,60336275 3
100	2,3	5	0,5	0,832909123	0,3985635 99	0,60143640 1
125	1,3	6	0,6063 82979	0,262364264	0,4000572 39	0,59994276 1
150	1,6	7	0,7127 65957	0,470003629	0,4012772 53	0,59872274 7
175	1,2	8	0,8191 48936	0,182321557	0,4023084 86	0,59769151 4
200	1,65	9	0,9255 31915	0,500775288	0,4032015 71	0,59679842 9

Table 3. Shannon Entropy F(t) and y(t) values calculated by equations 1, 2, 3, 4, 5, 6 and 7 for Tritium with 25keV bombardment with 3T on Graphene Crystal

Process Time (fs)	Shannon Entropy of the total bulk surface	Rank	F(t)	ln(Shannon)	y(t)_Shannon	Reliability of Shannon Entropy for 25keV Tritium Bombardment
0	5,2	1	0,0744 68085	1,6486 58626	0	1
25	4,85	2	0,1808 51064	1,5789 78705	0,5576 74481	0,44232 5519
50	4,8	3	0,2872 34043	1,5686 15918	0,5995 98835	0,40040 1165
75	4,4	4	0,3936 17021	1,4816 04541	0,6229 18871	0,37708 1129
100	3,95	5	0,5	1,3737 15579	0,6389 00742	0,36109 9258
125	3,5	6	0,6063 82979	1,2527 62968	0,6509 68528	0,34903 1472
150	3	7	0,7127 65957	1,0986 12289	0,6606 13268	0,33938 6732

175	2,5	8	0,8191 48936	0,9162 90732	0,6686 15827	0,33138 4173
200	0,65	9	0,9255 31915	-0,4307 82916	0,6754 3507	0,32456 493

Table 4. Shannon Entropy F(t) and y(t) values calculated by equations 1, 2, 3, 4, 5, 6 and 7 for Tritium with 35keV bombardment with 3T on Graphene Crystal

Process Time (fs)	Shannon Entropy of the total bulk surface	Rank	F(t)	ln(Shannon)	y(t)_Shannon	Reliability of Shannon Entropy for 35keV Tritium Bombardment
0	5,5	1	0,0744 68085	1,7047 48092	0	1
25	5,3	2	0,1808 51064	1,6677 06821	0,47404 3473	0,52595 6527
50	4,45	3	0,2872 34043	1,4929 04096	0,49735 5401	0,50264 4599
75	3,65	4	0,3936 17021	1,2947 27168	0,51078 1671	0,48921 8329
100	3,45	5	0,5	1,2383 74231	0,52020 5206	0,47979 4794
125	3,25	6	0,6063 82979	1,1786 54996	0,52745 3135	0,47254 6865
150	2,6	7	0,7127 65957	0,9555 11445	0,53333 388	0,46666 612
175	2,85	8	0,8191 48936	1,0473 18994	0,53827 6319	0,46172 3681
200	2,8	9	0,9255 31915	1,0296 19417	0,54253 5258	0,45746 4742

In the above tables ln(Shannon) column is used to calculate the values of y(t)\_Shannon columns based on the trendline functions slope equations given in (6). Then the last column is computed with the equation (3) to calculate the reliability of the materials based on the Shannon Entropy and the resultant graphs are given in the figures 5, 6, 7, 8:

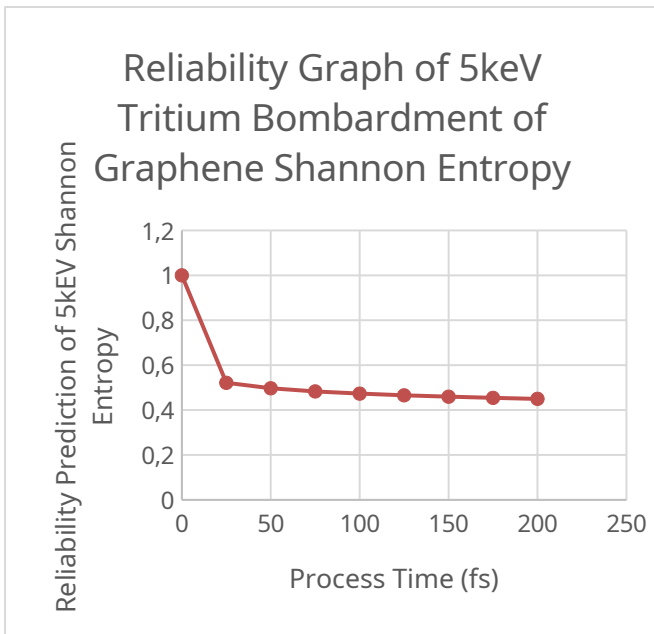


Figure 5. Calculated reliability of Shannon Entropy of the simulated system based on 5keV bombardment of Tritium.

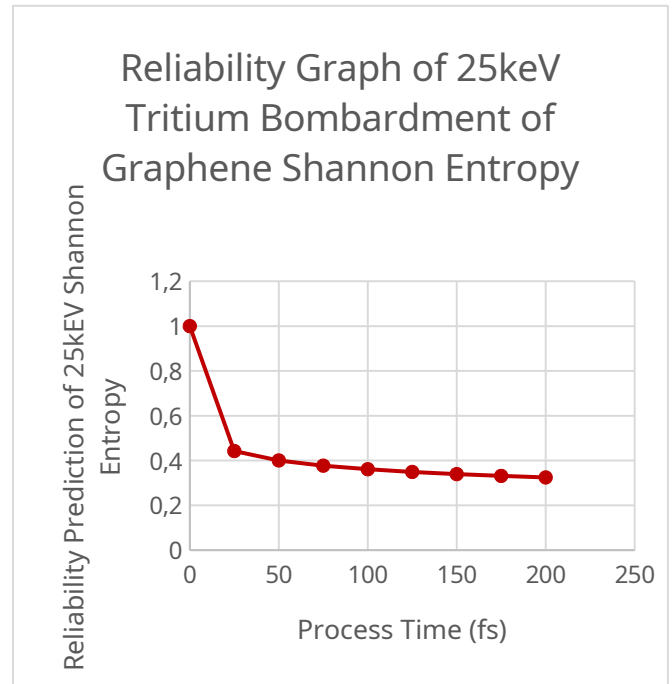


Figure 7. Calculated reliability of Shannon Entropy of the simulated system based on 25keV bombardment of Tritium.

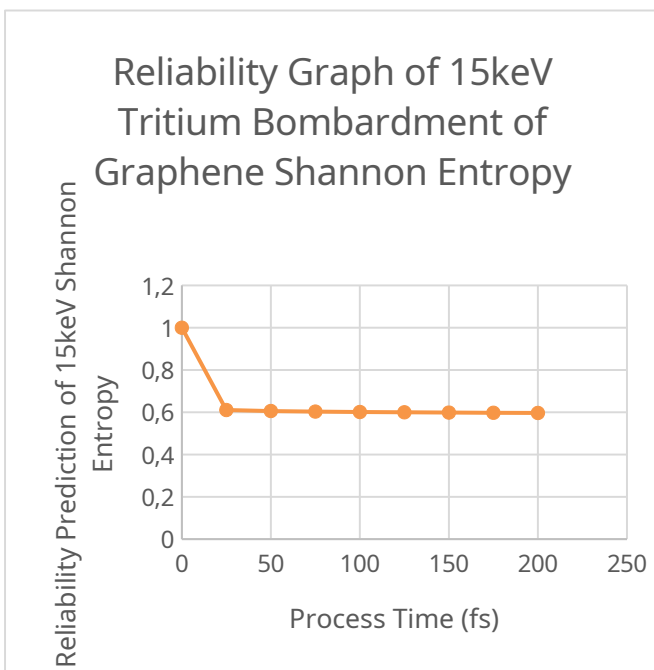


Figure 6. Calculated reliability of Shannon Entropy of the simulated system based on 15keV bombardment of Tritium.

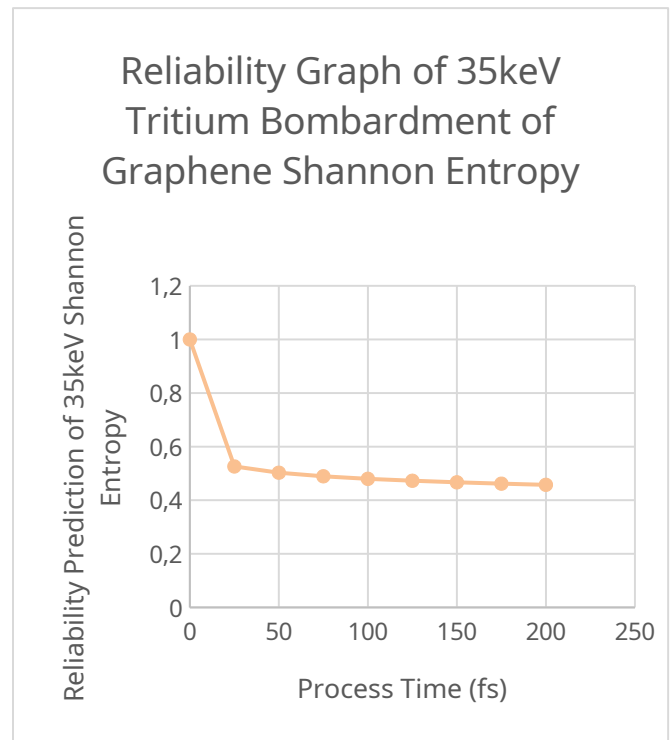


Figure 8. Calculated reliability of Shannon Entropy of the simulated system based on 35keV bombardment of Tritium.

Entropy of the simulated system based on 35keV bombardment of Tritium.

When the Figures 5,6,7,8 are observed both graphs show the similarity with the Weibull distribution probability density function of the hazard function. Since the Shannon Entropy is a measure of the chaos in information entropy, reliability of the material of the graphene crystal would be considered as low as given in the results section.

#### **4. CONCLUSION**

The graphs shown in the earlier results help evaluate the material choices needed for plasma-based energy devices, like fusion Tokamak reactors and space propulsion systems. The Weibull distribution, which uses calculations based on Shannon entropy, is a useful way to assess how reliable structures are when they interact with plasma and materials, as shown by the estimated results. The nuclear fission industry currently employs this technique for predicting structural reliability. Upcoming experiments will examine how collisions in plasma and the ability of graphene surfaces to hold onto tritium affect the material's reliability. This analysis indicates that the design of Tokamak fusion reactors with graphene surface tiles will be influenced by the tritium used in the plasma core to help keep it in

place. The simulation results indicated that graphene layers might hold onto more tritium because of the way carbon and hydrogen atoms interact with each other. This analysis indicates that the wall structures of Tokamak fusion reactors, including the European Union's International Thermonuclear Experimental Reactor (ITER), will utilize various materials, such as tungsten, instead of graphene.

#### **Declarations**

#### **Availability of Data and Material**

The article and supplementary materials substantiate the study's conclusions. Upon reasonable request, the corresponding author can furnish supplementary data pertaining to the specified study.

#### **Funding**

No funding is used for this simulation work only resource used is the computer resources are used as support.

#### **Authors' Contributions**

Author, developed the theoretical formalism, performed the analytic calculations and performed the numerical simulations. And also author is contributed to the final version of the manuscript.

#### **Acknowledgments**

This research article is being supported by the research and development department of Havelan

Inc.

## Conflict of Interest

No potential financial or non-financial conflicts of interest existed during the research. Furthermore, the study failed to obtain informed consent from human participants or animals while adhering to the ethical standards of globally recognized research and publication.

## References

- [1] Ongena J., "Nuclear fusion and its large potential for the future world energy supply", 2016, Nukleonika Journal, pp:425-432, web site ref: <https://sciendo.com/pdf/10.1515/nuka-2016-0070>
- [2] Takeda S., Pearson R. Nuclear Fusion Power Plants. Power Plants in the Industry. 2018; Chap 6: 101-122, IntechOpen publishing, website ref: <https://www.intechopen.com/chapters/62970>, DOI: 10.5772/intechopen.80241
- [3] IAEA. Fusion Energy for Peace and Sustainable Development. IAEA. Vienna. 2018: 2-18. web site ref: [https://nucleus.iaea.org/sites/fusionportal/SiteAssets/18-03925E\\_BRO\\_Fusion.pdf](https://nucleus.iaea.org/sites/fusionportal/SiteAssets/18-03925E_BRO_Fusion.pdf)
- [4] IAEA. Kikuchi M., Lackner K., Tran M. Q. Fusion Physics. Vienna. 2012: 20-21, web site ref: [https://wwwpub.iaea.org/MTC/D/Publications/PDF/Pub1562\\_web.pdf](https://wwwpub.iaea.org/MTC/D/Publications/PDF/Pub1562_web.pdf)
- [5] Ibrahim S., Lahboub F. Z., Brault P., Petit A., Caillard A., Millon E., Sauvage T., Fernandez A., Thomann A.L. Influence of helium incorporation on growth process and properties of aluminum thin films deposited by DC Magnetron sputtering. Surface and Coatings Technology. 2021; Vol; 426, web site ref: <https://www.sciencedirect.com/science/article/abs/pii/S0257897221009828>, <https://doi.org/10.1016/j.surfcoat.2021.127808>
- [6] Behrish R., Harries D. R. International Atomic Energy Agency. Lifetime Predictions For The First Wall and Blanket Structure of Fusion Reactors. Proceedings of a Technical Committee Meeting. Karlsruhe. Nuclear Fusion J. 1986; Vol: 26, DOI 10.1088/0029-5515/26/5/015
- [7] IoP Publishing Ltd. Nuclear Fusion Half a Century of Magnetic Confinement Fusion Research. 2002:230-258, web site ref: [https://library.psfc.mit.edu/catalog/online\\_pubs/conference%20proceedings/fusion%20energy%20conferences/Nuclear%20Fusion%20\(IOP\)%20half%20a%20century.pdf](https://library.psfc.mit.edu/catalog/online_pubs/conference%20proceedings/fusion%20energy%20conferences/Nuclear%20Fusion%20(IOP)%20half%20a%20century.pdf)
- [8] Jones E. S., Rafelski J. Cold Nuclear Fusion. Scientific American. Springer Nature Publishing. 1987: 66-71, web site ref: <https://www.fulviofrisone.com/attachments/article/358/Cold%20Nuclear%20Fusion.pdf>
- [9] Kajita S., Kawaguchi, Ohno N., Yoshida N. Enhanced growth of large-scale nanostructures with metallic ion precipitation in helium plasmas. Scientific Reports. Springer Nature. 2018. web site ref: [https://www.researchgate.net/publication/322315992\\_Enhanced\\_growth\\_of\\_large-scale\\_nanostructures\\_with\\_metallic\\_ion\\_precipitation\\_in\\_helium\\_plasmas](https://www.researchgate.net/publication/322315992_Enhanced_growth_of_large-scale_nanostructures_with_metallic_ion_precipitation_in_helium_plasmas), <https://doi.org/10.1038/s41598-017-18476-7>
- [10] Kotov V. Particle conservation in numerical models of the tokamak plasma edge. Physics Plasma Ph Archive. Forschungszentrum Jülich GmbH, Institut für Energie- und Klimaforschung-Plasmaphysic. Partner of the Trilateral Euregio Cluster. Jülich, Germany, 2017; Vol 24, <https://doi.org/10.1063/1.4980858>
- [11] K. Wojczykowski. New Development in Corrosion Testing: Theory, Methods and Standards. AESF Foundation, Plating and Surface Finishing. 2011; Vol January, web site ref: <https://www.pfonline.com/articles/new-developments-in-corrosion-testing-theory-methods-and-standards>
- [12] Linden T. Compact Fusion Reactors. CERN Colloquium. Helsinki Institute of Physics 2015; Vol March, web site ref: <http://cds.cern.ch/record/2004827>
- [13] L. Rajablou, S.M. Motevalli, F. Fadaei. Study of alpha particle concentration effects as the ash of deuterium-tritium fusion reaction on ignition criteria. Physica Scripta. 2022; Vol 97, No 9: DOI 10.1088/1402-4896/ac831a
- [14] Malo M., Morono A., Hodgson E. R. Plasma Etching to Enhance the Surface Insulating Stability of Alumina for Fusion Applications. Nuclear Materials and Energy. Elsevier. 2016; Vol 9: 247-250, DOI: 10.1016/j.nme.2016.05.008
- [15] Miyamoto K. Fundamentals of Plasma Physics and Controlled Fusion. 2011. 3rd Edition: 1-21, web site ref: <https://www.nifs.ac.jp/report/NIFS-PROC-88.pdf>, DOI 10.1088/0029-5515/38/4/701
- [16] Nadler J. Inertial-Electrostatic Confinement (IEC) of A Fusion Plasma with Grids. Nuclear Engineering Department, University of Illinois. 1995, web site ref: <http://sites.apam.columbia.edu/SMproceedings/11.ContributedPapers/11.Nadler.pdf>
- [17] Nordlund K. Atomistic Simulations of Plasma-wall interactions in Fusion Reactors. Physica Scripta. 2006; Vol T124:53-57, DOI 10.1088/0031-8949/2006/T124/011

[18] Ongena J., "Nuclear fusion and its large potential for the future world energy supply", 2016, Nukleonika Journal, pp:425-432, web site ref: <https://sciencedirect.com/pdf/10.1515/nuka-2016-0070>

[19] Perrault D. Nuclear Fusion Reactors-Safety and Radiation Protection Considerations for Demonstration Reactors that follow ITER facility. IRSN. 2017; Vol Nov: 15-27, web site ref: [https://www.irsn.fr/EN/Research/publications-documentation/ScientificBooks/Documents/ITER-VA\\_web\\_non\\_imprimable.pdf](https://www.irsn.fr/EN/Research/publications-documentation/ScientificBooks/Documents/ITER-VA_web_non_imprimable.pdf)

[20] Arena P., Maio P. A. Special Issue .Structural and Thermo-Mechanical Analysis in Nuclear Fusion Reactors. MDPI Applied Sciences. 2020; web site ref: [https://www.mdpi.com/journal/applsci/special\\_issues/Fusion\\_Reactors](https://www.mdpi.com/journal/applsci/special_issues/Fusion_Reactors), <https://doi.org/10.3390/app122412562>

[21] Apostolakis G. E., Sanzo D. L. Limiter Probabilistic Lifetime Analysis. Fusion Engineering and Design. 1988; Vol. 6:229-267, [https://doi.org/10.1016/S0920-3796\(88\)80111-X](https://doi.org/10.1016/S0920-3796(88)80111-X)

[22] Du, X. Unified Uncertainty Analysis by the First Order Reliability Method. J. Mech. Des. 2008; Vol 30 (9): 091401-09410, DOI:10.1115/1.2943295

[23] Freidberg J.P., Mangiarotti F.J., Minervini J. Designing a Tokamak Fusion Reactor-How Does Plasma Physics Fit In?. Plasma Science and Fusion Center. Massachusetts Institute of Technology, Cambridge MA. 2015; Vol June; 16., <https://doi.org/10.1063/1.4923266>

[24] Fusion Energy Sciences Workshop. On Plasma Material Interactions-Report on Science Challenges and Research Opportunities in Plasma Material Interactions. U.S. Department of Energy, Office of Science, Fusion Energy Sciences, 2015

[25] Ask Hjorth Larsen, Jens Jørgen Mortensen, Jakob Blomqvist, Ivano E. Castelli, Rune Christensen, Marcin Dułak, Jesper Friis, Michael N. Groves, Bjørk Hammer, Cory Hargus, Eric D. Hermes, Paul C. Jennings, Peter Bjerre Jensen, James Kermod, John R. Kitchin, Esben Leonhard Kolsbjerg, Joseph Kubal, Kristen Kaasbjerg, Steen Lysgaard, Jón Bergmann Maronsson, Tristan Maxson, Thomas Olsen, Lars Pastewka, Andrew Peterson, Carsten Rostgaard, Jakob Schiøtz, Ole Schütt, Mikkel Strange, Kristian S. Thygesen, Tejs Vegge, Lasse Vilhelmsen, Michael Walter, Zhenhua Zeng, Karsten Wedel Jacobsen, "The Atomic Simulation Environment—A Python library for working with atoms", Phys.: Condens. Matter Vol. 29 273002, 2017

[26] Karaca Y, Moonis M., "Multi-Chaos, Fractal and Multi-Fractional Artificial Intelligence of Different Complex Systems", Chapter 14, pp:231-245, Academic Press, 2022

[27] K. Wojcyskowski. New Development in Corrosion Testing: Theory, Methods and Standards. AESF Foundation, Plating and Surface Finishing. 2011; Vol January, web site ref: <https://www.pfonline.com/articles/new-developments-in-corrosion-testing-theory-methods-and-standards>